Parasitology Research (2019) 118:3429–3441
https://doi.org/10.1007/s00436-019-06471-y

IMMUNOLOGY AND HOST-PARASITE INTERACTIONS - ORIGINAL PAPER

Cryptosporidium parvum alters glucose transport mechanisms in infected enterocytes

Cora Delling[1] · Arwid Daugschies[1,2] · Berit Bangoura[3] · Franziska Dengler[4]

Received: 9 May 2019 / Accepted: 24 September 2019 / Published online: 31October 2019
© Springer-Verlag GmbH Germany, part of Springer Nature 2019

Abstract

The parasite *Cryptosporidium parvum* Tyzzer 1912 destroys parts of the intestinal brush border membrane which is important for the uptake of nutrients like glucose. In this study, glucose transport mechanisms of the host cells (IPEC-J2 cells) infected by *C. parvum* were investigated. The mRNA expression levels of glucose transporters (GLUT) 1 and 2 and Na^+-coupled glucose transporter (SGLT) 1 were compared in infected and uninfected cells over an infection time of 24–96 h by RT-qPCR. Furthermore, the protein expression of SGLT 1 and GLUT 2 was quantified in western blot studies. While the protein expression of SGLT 1 was not altered in infected cells, mRNA expression of SGLT 1 and GLUT 1 was significantly increased 24 h p. i. and decreased 96 h p. i. The mRNA expression of GLUT 2 was significantly decreased 24 h, 72 h, and 96 h p. i. and also correlated significantly with the infection dose at 72 h p. i. In contrast to that, the protein expression of GLUT 2 was significantly increased 48 h p. i., associated with a significantly higher intracellular glucose level in infected cells compared with control cells at that time point of infection. This points to an adaptation of the host cells' glucose uptake taking place in the acute phase of the infection. A better understanding of these molecular mechanisms following a *C. parvum* infection may probably lead to an improvement of therapy strategies in the future.

Keywords *C. parvum* infection · Glucose transport · IPEC-J2 cells · Parasite-host interaction

Introduction

The protozoan *Cryptosporidium parvum* Tyzzer 1912 causes enteropathies in humans and animals all over the world. In immunocompetent hosts, cryptosporidiosis is a self-limiting disease leading to a highly variable severity of symptoms. Children in developing countries are especially exposed and can suffer from severe diarrhea in case of infection (Kotloff et al. 2013; Platts-Mills et al. 2015). Furthermore, cryptosporidiosis is an important parasitosis of domestic animals adversely affecting the animal welfare and causing economic losses especially in calves (Lendner et al. 2011), and is often associated with bacterial or viral infections (Göhring et al. 2014). By now, there is no drug available which eliminates the parasites or suppresses the symptoms completely.

After the invasion of intestinal epithelial cells, the parasite employs the host cell metabolism, exploiting it for nutrients in order to survive and multiply (Lendner and Daugschies 2014). After asexual and sexual replication, parasite stages leave the host cells supposedly by induction of host cell apoptosis (Sasahara et al. 2003; Foster et al. 2012), thereby damaging the intestinal epithelium and causing atrophy of intestinal villi (Drinkall et al. 2017). The gastrointestinal epithelium is characterized by the formation of a barrier to potentially harmful agents in the intestinal lumen on the one hand but also by the mediation of directed transport across the epithelium on the other hand. Especially the small intestine plays a crucial role

Section Editor: Lihua Xiao

✉ Cora Delling
cora.delling@vetmed.uni-leipzig.de

[1] Institute of Parasitology, Faculty of Veterinary Medicine, University of Leipzig, An den Tierkliniken 35, 04103 Leipzig, Germany

[2] Albrecht Daniel Thaer Institute, An den Tierkliniken 29, 04103 Leipzig, Germany

[3] Wyoming State Veterinary Laboratory, Department of Veterinary Sciences, University of Wyoming, 1174 Snowy Range Road, Laramie, WY 82070, USA

[4] Institute of Veterinary Physiology, Faculty of Veterinary Medicine, University of Leipzig, An den Tierkliniken 7, 04103 Leipzig, Germany

in the uptake of nutrients, e.g., glucose and galactose derived from lactose, the main energy source for suckling mammals.

This uptake is considered to be mediated almost exclusively by the Na^+/glucose cotransporter (SGLT 1) (Wright et al. 2003), which is located in the brush border membrane. At the basolateral membrane, the release of the hexoses into the bloodstream is mediated via facilitated diffusion mainly by glucose transporter (GLUT) 2 (Kellett et al. 2008; Chen et al. 2016). A related transporter, GLUT 1, is found in most mammalian cells and transports monosaccharides and vitamin C (Bürzle and Hediger 2012). GLUT 1 features a widespread intracellular distribution in normal jejunal epithelial cells that are not exposed to stressors (Boyer et al. 1996). However, this transporter model seems to be susceptible to changes under pathological circumstances. For example, several studies demonstrate a recruitment of GLUT 2 to the apical membrane under special conditions like high luminal glucose or stress (Kellett et al. 2008; Krimi et al. 2009; Steinhoff-Wagner et al. 2014). Thus, an infection with *C. parvum* might initiate a similar adaptation to sustain the cellular viability and thus epithelial integrity. Since the major energy source of intracellular *C. parvum* stages are sugars like glucose that are scavenged from the enterocyte and utilized by glycolysis (Rider and Zhu 2010), and the parasite is able to manipulate the host cell by secreting molecules into it (Lendner and Daugschies 2014), it might also be possible that an adaptation of intestinal glucose transport mechanisms could be used as an infection strategy by *C. parvum* in infected cells.

A potential influence on glucose transporter reorganization in host cells caused by *C. parvum* infection could be a promising therapeutic approach, and knowledge about the molecular mechanism of infectious diarrheal disease can lead to advances in targeted therapies or repurpose existing agents (Das et al. 2018). Thus, a first step towards this would be the confirmation of the transporters involved in this reorganization and their respective roles in the glucose import into infected enterocytes. In the present study, the influence of *C. parvum* infection on the glucose transport capacities of enterocytes was evaluated with regard to intracellular glucose levels and the expression of different glucose transporter in vitro.

Material and methods

Parasites

The in-house strain of *C. parvum* (LE-01-Cp-15) was used in all experiments. The strain was passaged every 3 months in neonatal calves, and freshly recovered oocysts were isolated and stored as described earlier (Najdrowski et al. 2007; Dresely et al. 2015). Before use, oocysts were bleached for 5 min on ice with NaOCl (Roth, Karlsruhe, Germany) (4%) and centrifuged for 7 min at 6300×*g*. Afterwards, oocysts were washed with phosphate buffered saline (PBS; Life Technologies GmbH, Darmstadt, Germany) once and centrifuged again. Then oocysts were resuspended in 1 mL growth medium (see below) and counted in a Neubauer chamber.

Cell culture

For all experiments, IPEC-J2 cells (passage 35–55), a kind gift by the Institute of Cell Biology and Physiology, University of Veterinary Medicine Hannover, Foundation were used. 2×10^5 IPEC-J2 cells per well were seeded in 24 well plates and covered with growth medium consisting of IMDM, supplemented with F-12 (1×) + GlutaMAX™-I, 5 % fetal calf serum (FCS), and L-glutamine 200 mM (media and all reagents: Life Technologies GmbH, Darmstadt, Germany). After attaining confluence, cells were infected with 1.5×10^5, 3×10^5 or 6×10^5 oocysts, respectively, and covered with infection medium consisting of growth medium plus 0.4 % sodium taurocholate (Sigma-Aldrich, Munich, Germany), 0.5 % gentamycin (Biochrom, Berlin, Germany), and 1 % amphotericin B (Biochrom, Berlin, Germany). The infected cells were centrifuged for 5 min at 200×*g*. Thereafter, infected monolayers were incubated for 3 h at 37 °C and 5 % CO_2. Then the monolayer was washed twice using PBS and covered again with growth medium and antibiotics (0.5 % gentamycin and 1 % amphotericin B). At 24, 48, 72, and 96 h p. i., cells were harvested using trypsin (Biochrom, Berlin, Germany). Uninfected cells and cells infected by heat inactivated oocysts (70 °C, 30 min) served as control for infection analyses. DNA-extraction and quantitative real-time PCR (qPCR) for detecting Cp-hsp70 were performed as described before (Delling et al. 2017) in order to determine the success of infection. Three independent experiments were performed, with three wells for each control (uninfected and heat-inactivated oocysts) and each infection dose. Cultures were monitored by light microscopy using a Leica DM IL LED Fluo (Leica Microsystems CMS GmbH, Wetzlar, Germany) in 24 h intervals over the period of 96 h p. i. to observe morphological changes of the host cells.

Confocal laser scanning microscopy

8×10^4 IPEC-J2 cells were seeded in 8 well chamber slides (ibidi GmbH, Gräfelfing, Germany) and covered with growth medium. Cells were infected with 1.5×10^5 oocysts as described above. At 48 h p. i., cells were washed two times with PBS on ice and fixed with 4% paraformaldehyde (Roth, Karlsruhe, Germany) for 15 min at room temperature. Fixed cell cultures were washed twice with PBS and pre-incubated in PBS containing 4% horse serum (C.C. pro GmbH, Lörrach, Germany) and 0.1 % Triton X-100 (Sigma-Aldrich, Munich,

Germany). This solution was also used for the dilution of all antibodies. Then the slides were incubated with primary antibodies for SGLT 1 and GLUT 2 (see Table 1) for 2 h at room temperature. After washing thrice with PBS, the slides were incubated with the secondary antibodies and Sporo-glo™ (Waterborne, Inc., New Orleans, USA) (Table 1) for 1 h. For nuclear staining, DAPI was added (1:4000; Sigma Aldrich, Munich, Germany) for 1 min. Finally, the slides were mounted using glycerol-gelatin (Sigma Aldrich, Munich, Germany) and assessed using a Leica TCS SP8. The wells, in which only secondary antibody was used, served as control for unspecific binding of the secondary antibodies. Three-dimensional images were fashioned using the IMARIS 9.3 program (Bitplane, Oxford Instruments).

Two-step real-time reverse transcriptase polymerase chain reaction

At 24, 48, 72, and 96 h p. i., two wells each of control cells, i.e., uninfected cells, or cells infected with 1.5×10^5 oocysts were harvested from a 24 well plate by using BLTG lysis buffer from the ReliaPrep™ RNA Cell Miniprep System (Promega GmbH, Mannheim, Germany) and pooled to one sample after washing with Mg-free PBS once. At least 3 independent experiments of each time point were performed and examined for mRNA expression of glucose transporters [SGLT 1: $N = 4$ (24 h), 6 (48 h), 3 (72 h), 3 (96 h); GLUT 2: $N = 5$ (24 h), 7 (48 h), 4 (72 h), 3 (96 h); GLUT 1: $N = 4$ (24 h, 72 h), 7 (48 h), 3 (96 h)]. Total RNA was isolated using the ReliaPrep™ RNA Cell Miniprep System (Promega GmbH, Mannheim, Germany) according to the manufacturer's protocol including treatment with DNase. The RNA concentration and quality were determined with the aid of a spectrophotometer (BioPhotometer, Eppendorf, Wesseling-Berzdorf, Germany). Complementary DNA (cDNA) was synthesized from 1 μg RNA using the GoScript® Reverse Transcription System (Promega GmbH, Mannheim, Germany) according to the manufacturer's protocol. Quantitative real-time PCR was conducted using the GoTaq DNA Polymerase kit (Promega GmbH, Mannheim, Germany), 112 nM primer mix and DNase-free water as described by Dengler et al. (2018). The primer sequences and conditions for qPCR are shown in Table 2. A no template control (NTC) with DNase-free water instead of cDNA was applied for each run along with a negative control using RNA instead of cDNA to test each sample for genomic DNA. Quantitative real-time PCR reactions for each sample and gene were run in duplicate (i.e., two technical replicates) to minimize dispensation artifacts. The deviation of C_t of the technical replicates was < 0.3. If it was higher, data was discarded, and the run was repeated.

The primers were designed with the primer BLAST tool according to known sequences from the Basic Local Alignment Search Tool (BLAST) in the gene bank database of the National Center for Biotechnology Information (NCBI, Bethesda, MD, USA) and synthesized by Eurofins MWG (Ebersberg, Germany) (see Table 2). The amplicons were sequenced again, and the product sequences were verified by BLAST. The quantification cycle and amplification efficiency of each amplification curve were determined using the Rotor Gene 6000 Series Software 1.7 (Corbett/Qiagen Inc., Hilden, Germany). For analysis of the data, the 'Relative expression software tool' (REST 2009-RG Mode, Qiagen Inc., Hilden, Germany) established by Pfaffl et al. (2002) was used to calculate the relative mRNA expression with reference to that in uninfected cells, whose mRNA expression was set to 1. Thus, the mRNA expression in the infected cells is reported as a multiple of the control group. The C_t values set by the software were applied after checking them optically. Normalization of the samples was achieved by using the same amounts of cells and RNA for processing and by normalizing the data for the target genes with the aid of the reference genes YWHAZ and ribosomal protein (RP) L4. These genes have been proven to be stable under the experimental conditions applied in our study. Their stability was tested using the programs BestKeeper© (version 1 by M.W. Pfaffl, Institute of Physiology, Center of Life and Food Sciences, TUM-Weihenstephan, Germany, 2004) and geNorm (Vandesompele et al. 2002).

Table 1 Antibodies used for CLSM

Target	SGLT 1	GLUT 2	*C. parvum*
Primary antibody	Rabbit-anti-SGLT 1	Goat-anti-GLUT 2	Sporo-glo™, Cy3-labeled Rat-anti-*C. parvum* sporozoite
Manufacturer/catalog number	Antibodies online/ABIN364451	Santa Cruz Biotechnology/sc-7580	Waterborne Inc/A600Cy3R-1X
Dilution	1:100	1:100	Working solution 1:5
Secondary antibody	Donkey-anti-rabbit ALEXA 488	Donkey-anti-goat ALEXA 488	-
Manufacturer/catalog number	Jackson Immuno Research Laboratories, Inc. / 711-545-152	Fisher Scientific/Invitrogen A11055	-
Dilution	1:200	1:200	-

Table 2 Primers used for qPCR to quantify mRNA expression levels of glucose transporters

Gene	GenBank accession number	30 s annealing temp. (°C)	Amplicon size (bp)	Sequence (5–3′)
RPL4	XM_005659862.3	58	92	F: GCACCACGCAAGAAGATTCA
				R: TGTCTTTGCATACGGGTTTAGC
GLUT1	KU672521	59	108	F: GGTTCATTGTGGCCGAACTC
				R: TACTGGAAGCACATGCCCAC
GLUT2	NM_001097447	59	91	F: TGCTCCAACCAAGTTCAGGG
				R: AGTCGAGGCCTATGATCTGAC
SGLT1	NM_001164021	60	89	F: TCACCAGTTACTTGGGACCAC
				R: GTCCCCAAAAGGCTCCCTCC
YWAHZ	NM_001315726.1	58	87	F: GGCCCTTAACTTCTCTGTGTT
				R: GGCTTCATCAAATGCTGTCT

Western blot analysis

For western blot, two wells each of control cells or infected cells (each well infected with 1.5×10^5 oocysts) were harvested from a 24 well plate at 24, 48, 72, and 96 h p. i. Both wells were homogenized together in 500 μL of a RIPA lysis buffer (Amresco, LLC, VWR, Solon, USA) with protease and phosphatase inhibitors (100X Halt™ protease and phosphatase inhibitor cocktail, Thermo Fisher Scientific, Schwerte, Germany). Five independent experiments were performed ($N = 5$). The protein concentration was measured using the bicinchoninic acid (BCA) method with a Tecan Spectra Rainbow Microplate Reader (Tecan Deutschland GmbH, Crailsheim, Germany) and bovine serum albumin (BSA) as standard. These protein samples were used for separation by sodium dodecyl sulfate-polyacrylamide gel electrophoresis (SDS-PAGE; 6 μg protein per well). After that, the samples were transferred onto a nitrocellulose membrane (Roth, Karlsruhe, Germany) using the Mini-Protean© system (Bio-Rad Laboratories Inc., Munich, Germany). The membrane was preincubated in 5% skim milk in Tris-buffered saline containing 0.2% Tween-20 (TBST) at 4 °C overnight. On the next day, it was incubated with the primary antibodies (Table 3) at room temperature with gentle shaking for 2 h. After washing five times with TBST, the membranes were incubated with a HRP-coupled secondary antibody (Table 3) at room temperature with gentle shaking for 1 h. Subsequently, the membranes were rinsed again with TBST five times and once with TBS, then the signal was detected by enhanced chemiluminescence using a G:BOX Chemi XT4 (Syngene, Cambridge, UK) and analyzed with the GeneTools© software (Syngene, Cambridge, UK). β-Actin was used as a loading control in each blot. For each experiment ($N = 5$), two technical replicates were conducted.

Analysis of intracellular glucose levels

For examining the intracellular glucose level in infected and control cells, the Glucose-Glo™ Assay (Promega GmbH, Mannheim, Germany) was used. Cells were seeded in 24 well plates and the infection was performed as described above. After 24, 48, 72, and 96 h, infected cells as well as uninfected cells (one well each) were placed on ice and washed twice with ice-cold PBS. Afterwards, cells were covered with a mixture of PBS and inactivation solution (stock solution: 0.6 N HCl) (2:1) and shaken for 5 min following the manufacturer's instructions. After neutralization (stock solution: 1 M Tris) (3:1), cell lysates were transferred into tubes and Glucose Detection Reagent was added, and incubated for 1 h before analysis. The luminescence was recorded using a GloMax® 96 Microplate Luminometer (Promega GmbH, Mannheim, Germany). The experiment was performed eight times ($N = 8$).

Statistics

Unless stated otherwise, the results are described as arithmetic means ± standard error of mean (SEM). The significance is

Table 3 Antibodies used for western blot

Target	Primary antibody	Manufacturer/catalog number	Dilution	Secondary antibody	Manufacturer/catalog number	Dilution
SGLT 1	Rabbit-anti-SGLT 1	Antibodies online/ABIN364451	1:1000	Donkey-anti-rabbit HRP	Santa Cruz Biotechnology/sc-2077	1:5000
GLUT 2	Rabbit-anti-GLUT 2	Thermo Fisher Scientific/PA5-77459	1:200	Donkey-anti-rabbit HRP	Santa Cruz Biotechnology/sc-2077	1:5000
β-Actin	Mouse-anti-β-Actin	Santa Cruz Biotechnology/sc-47778	1:1000	Goat-anti-mouse HRP	Invitrogen/A16072	1:5000

expressed as the probability of error (p). *N* represents the number of biological replicates for each treatment. The data were pooled for statistical analysis. To check the normality of the data, the Shapiro-Wilk test was performed. Thereafter, the differences between the mean values of two or more groups were tested using the paired Student's *t* test or repeated measures one-way analysis of variance (ANOVA) with a subsequent Holm-Sidak test as appropriate (Sigma Plot 13.0, Systat Software Inc., Erkrath, Germany). The differences were assumed to be statistically significant if $p < 0.05$. Correlation was examined using the Pearson product-moment correlation test (Sigma Plot 13.0, Systat Software Inc., Erkrath, Germany).

Results

Validity of the infection model

To examine the influence of *C. parvum* on the host cells' glucose transport, an infection model was established in IPEC-J2 cells. The infection was quantified by qPCR (Fig. 1). There was a peak of infection 48 h after inoculation as measured by the quantity of Cp-hsp70 gene copies. At 72 h and 96 h p. i., the level of infection was comparable to infection 24 h after inoculation. Additionally, the integrity of the monolayers was confirmed microscopically over the infection time of 96 h.

mRNA expression levels of SGLT 1, GLUT 1, and GLUT 2

The mRNA expression of SGLT 1 showed a varying trend over time. Initially at 24 h p. i., expression of SGLT 1 was significantly upregulated compared with control cells ($p < 0.001$). Thereafter, it decreased gradually until 96 h p. i., when its expression was significantly downregulated ($p < 0.01$; Fig. 2a). Higher infection doses showed no effect on SGLT 1 mRNA expression as measured at 72 h p. i. (Fig. 2b). The mRNA expression of GLUT 1 was significantly upregulated 24 h p. i. compared with control cells ($p < 0.05$) (Fig. 2c). However, at both 48 h and 72 h p. i., no significant difference between control and infected cells was detectable. Even higher infection doses did not influence the mRNA expression of GLUT 1 at 72 h p. i. (Fig. 2d). In comparison, the mRNA expression of GLUT 2 was significantly downregulated at all time points p. i. over a period of 96 h ($p < 0.001$), except for 48 h p. i. (Fig. 2e). Furthermore, the downregulation of GLUT

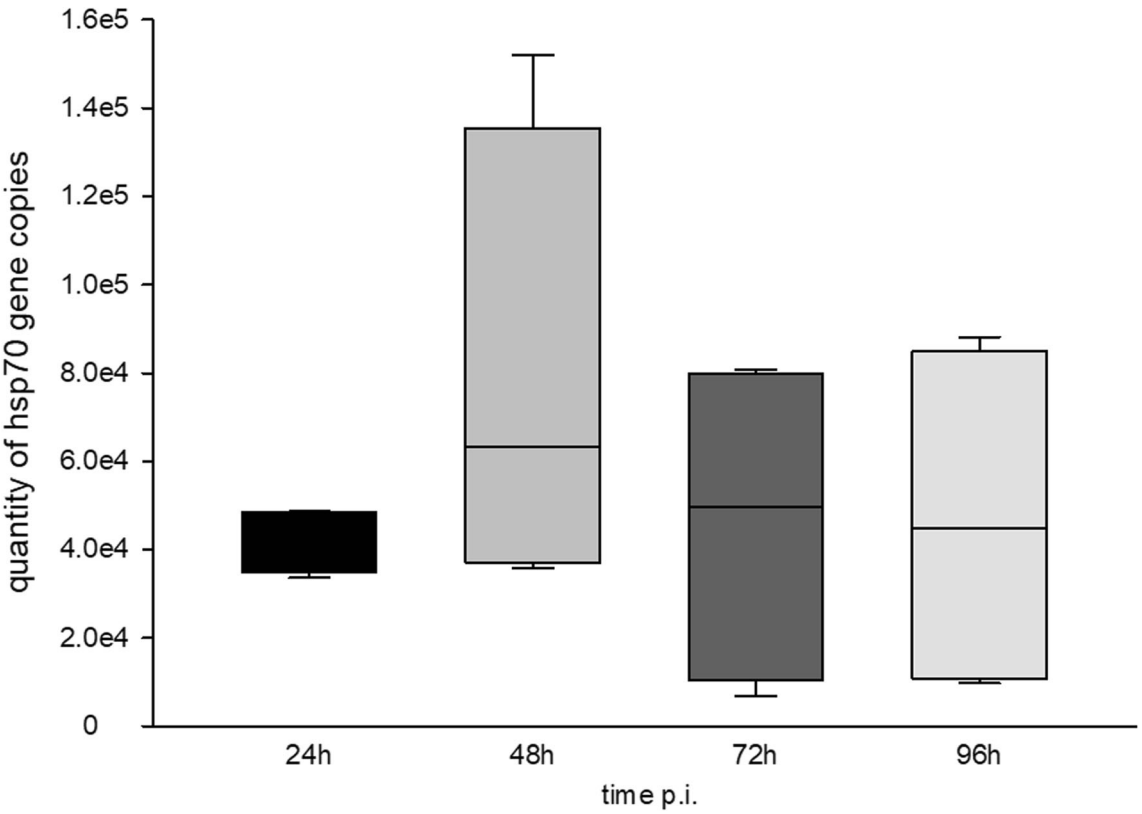

Fig. 1 Quantification of Cp-hsp70 gene copies after infection of IPEC-J2 cells over a time period of 96 h; data represent the results of three independent experiments with three replicates per cell culture each; boxes represent the median with the 10th, 25th, 75th, and 90th percentile as error bars

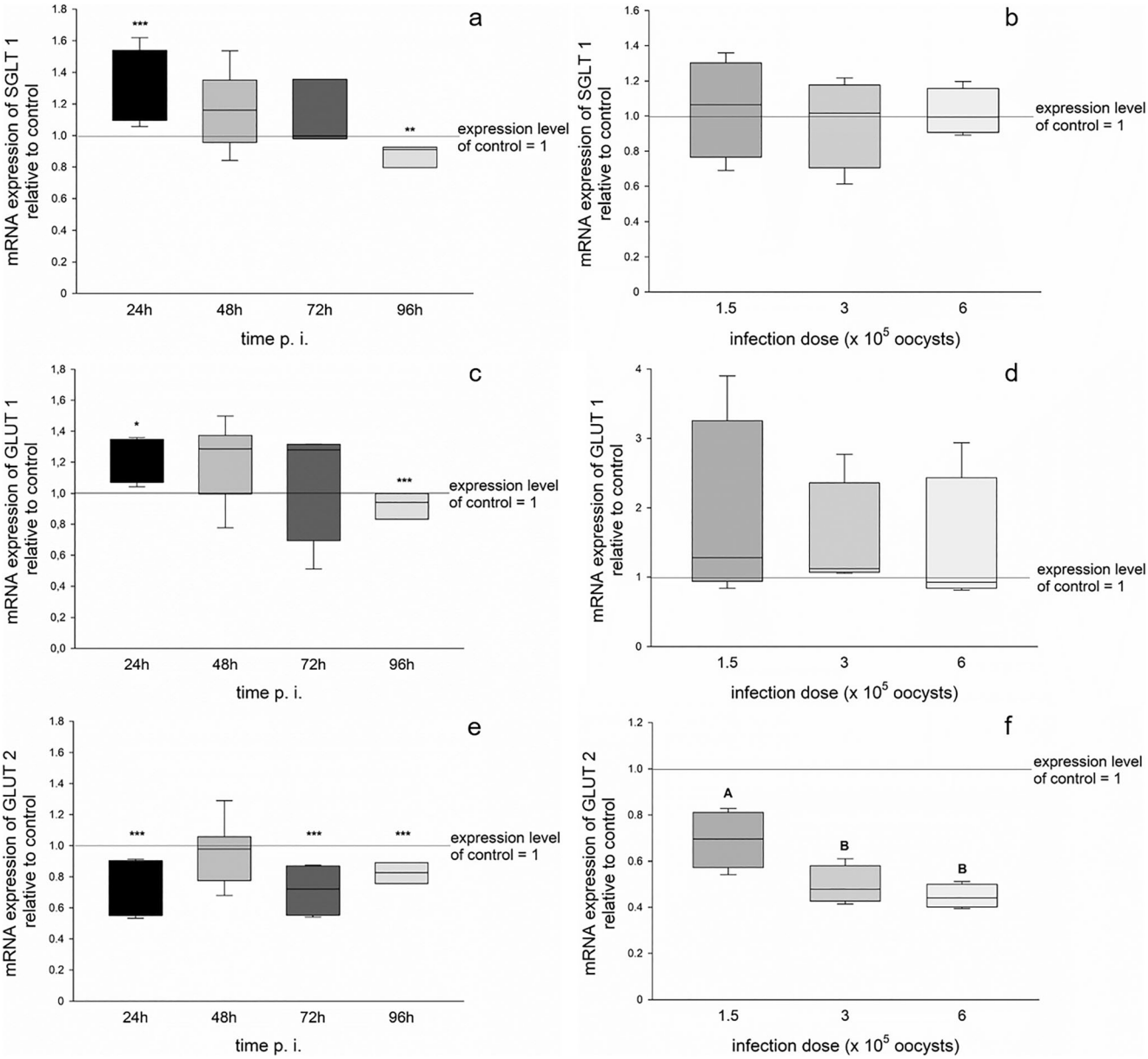

Fig. 2 Relative mRNA expression of glucose transporters in infected IPEC-J2 cells compared with control cells (expression levels of uninfected controls were set to 1, as indicated by the horizontal base line); box plots: median, inner line; box limits, 25th/75th percentile; bars, 10th/90th percentile. **a** SGLT 1: $N = 4$ (24 h), 6 (48 h), 3 (72 h), 3 (96 h). **b** SGLT 1 expression 72 h p. i. using several infection doses; $N = 4$. **c** GLUT 1: $N = 4$ (24 h, 72 h), 7 (48 h), 3 (96 h). **d** GLUT 1 expression 72 h p. i. using different infection doses; $N = 4$. **e** GLUT 2: $N = 5$ (24 h), 7 (48 h), 4 (72 h), 3 (96 h). **f** GLUT 2 expression 72 h p. i. using different infection doses; $N = 4$ (3×10^5, 6×10^5), 6 (1.5×10^5); for statistical analysis of **a**, **c**, and **e**, Student's test was used compared with control (*$p < 0.05$, **$p < 0.01$, ***$p < 0.001$); for statistical analysis of **b**, **d**, and **f**, one-way RM ANOVA was used ($p < 0.01$; different letters indicate significant differences between the groups)

2 showed a highly significant correlation to the infection dose at 72 h p. i. ($r^2 = 0.71$; $p < 0.0001$) (Figs. 2f and 3).

Protein expression of SGLT 1 and GLUT 2

While the protein expression, detected by western blot, was not altered in infected cells compared with control cells at all time points for SGLT 1 (Fig. 4a), the protein expression of GLUT 2 was significantly higher in infected cells 48 h p. i. ($p < 0.05$) (Fig. 4b).

CLSM revealed no prominent changes in SGLT 1 localization in infected cells compared with control cells (Fig 5a, b). A predominant membrane localization of GLUT 2 protein could be observed in uninfected cells, while in infected cells, the transporter seemed to be increasingly localized in the cytoplasm (Figs. 5 and 6).

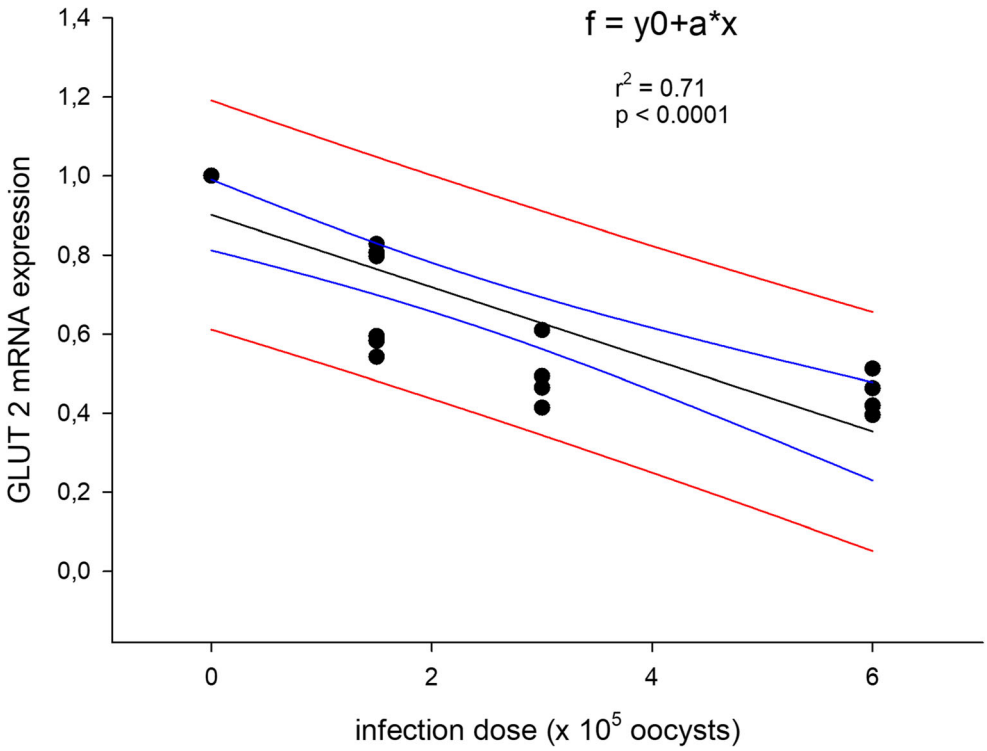

Fig. 3 Linear correlation between GLUT 2 mRNA expression and the infection dose (1.5×10^5, 3×10^5, 6×10^5) at 72 h p. i. ($r^2 = 0.71$; $p < 0.0001$)

GLUT 1 could not be detected on the protein level with commercially available antibodies.

Intracellular glucose levels

At 24 h p. i., no significant differences could be observed between the glucose level in infected and control cells (Fig. 7). After 48 h of infection, the infected cells showed a significantly higher intracellular glucose level than control cells ($p < 0.01$). At 72 h and 96 h p. i., the glucose level in infected cells was still higher than in control cells, although this was not statistically significant ($p = 0.056$ and $p = 0.086$, respectively).

Discussion

In *C. parvum* infection, a better understanding of the mechanisms of infection as well as the cellular response by the host might help to improve therapeutic approaches in mammalian hosts such as humans and domestic animals. Thus, the aim of this study was to investigate features related to glucose transport in intestinal epithelial cells infected with *C. parvum*. The main function of the intestinal epithelium is a directed transport of nutrients, electrolytes, and water from the gut lumen into the blood and vice versa. An important part of this directed transport is dedicated to the uptake of hexoses like glucose, serving as energy source for the host organism. It has been reported before, that especially this uptake of glucose into the enterocytes is strongly regulated under potentially noxious conditions, e.g., stress, hypoxia, or inflammation (Shepherd et al. 2004; Kellett et al. 2008; Krimi et al. 2009; Dengler et al. 2017) and can also be modulated due to parasitic infection (Sekikawa et al. 2003). Thus, we examined the potential impact of *C. parvum* infection on the glucose transporters SGLT 1, GLUT 1, and GLUT 2 as well as the intracellular glucose level in host cells.

So far, most *in vitro* studies on *C. parvum* were conducted in cell lines that are not primary natural target cells for this parasite. Additionally, most of them differ greatly in their features from small intestinal epithelial cells and are unsuitable for functional studies. Therefore, we used an infection model with non-transformed porcine IPEC-J2-cells for this study. This epithelial cell line was isolated from neonatal piglet jejunum by Helen Berschneider (Berschneider 1989) and has been characterized in detail by Schierack et al. (2006). The success of parasite invasion was ensured by qPCR (Fig. 1), confirming other studies (Mirhashemi et al. 2018; Ferguson et al. 2019) which demonstrated the general suitability of IPEC-J2 cells for cryptosporidiosis studies. As described by previous studies (Ferguson et al. 2019), a peak of infection at 48 h p. i. was detected by quantification of Cp-hsp70 gene copies.

After internalization, *C. parvum* is located intracellularly, but extracytoplasmatically in the host cells, i.e., intestinal epithelial cells, (Leitch and He 2012) and thus, the parasite is separated from the host cell cytoplasm by a parasitophorous vacuole (O'Hara and Chen 2011). *C. parvum* differs from other apicomplexans by the

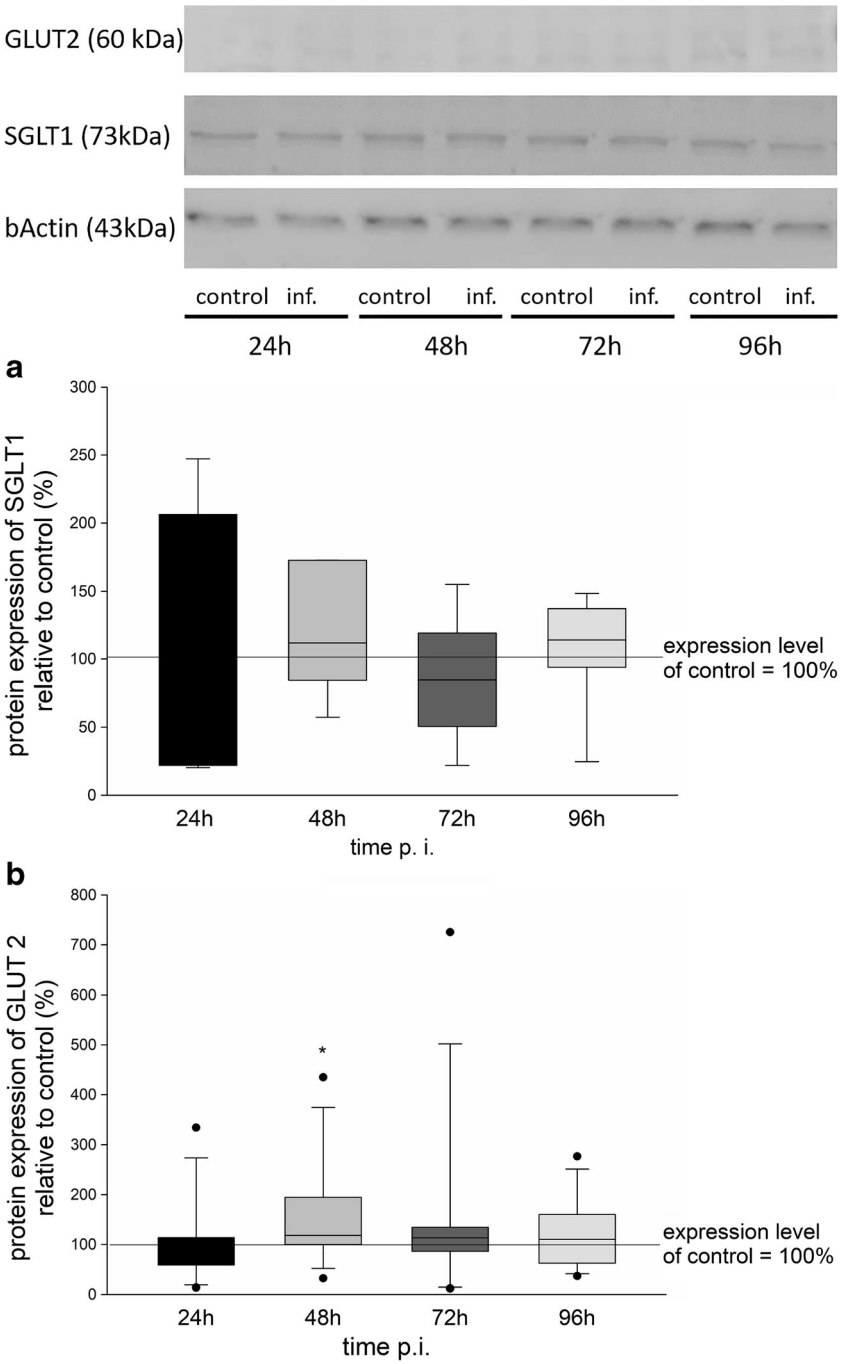

Fig. 4 Relative protein expression of **a** SGLT 1 and **b** GLUT 2 in IPEC-J2 at 24, 48, 72, and 96 h p. i. with 1.5×10^5 oocysts cells compared with control cells (expression was set to 100%, as indicated by the horizontal base line) analyzed by western blot; β-Actin was used as a loading control as exemplified in the image below; the boxes represent the median with the 10th, 25th, 75th, and 90th percentile as error bars; Student's test was used ($*p < 0.05$), and data represents the results of 5 biological replicates per time point

absence of many important metabolic pathways as well as its incapability for de novo synthesis of essential compounds (Yu et al. 2014). Therefore, a direct access to the host cells' nutrients is necessary for this parasite and it is assumed that this is ensured by a structure often referred to as the feeder organelle (Leitch and He 2012). Earlier studies postulated that glucose is important for the growth of *C. parvum* and the parasite might interfere with the host cells' glucose metabolism, e.g., by initiating an enhanced nutrient uptake by the host cell to ensure the survival and development of intracellular stages, comparable with the parasite's ability to manipulate apoptosis of infected epithelial cells to complete its life cycle (Liu et al. 2009). In this study, a significantly higher glucose level was detected 48 h p. i. in infected cells compared with control cells (Fig. 7), supporting this hypothesis.

Glucose and galactose are actively transported across the intestinal brush border membrane by SGLT 1, a secondary active high-affinity, low capacity transporter (Lehmann and Hornby 2016). Previously, it has been demonstrated that

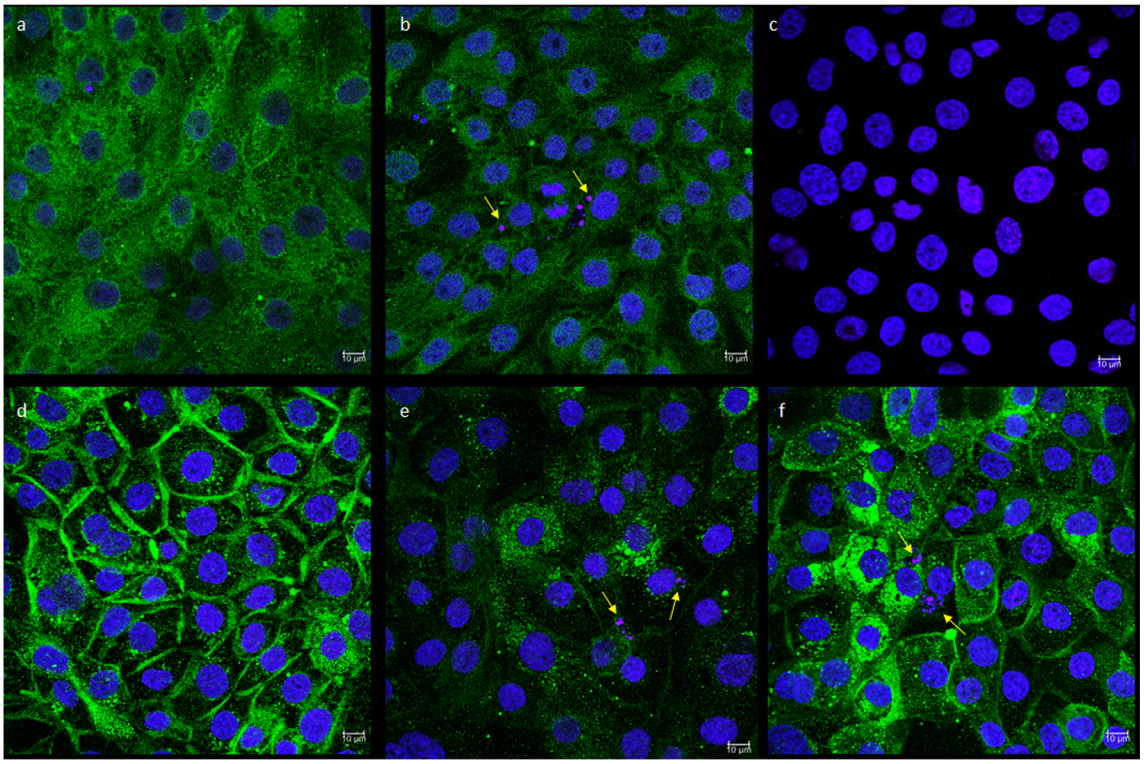

Fig. 5 Qualitative staining of SGLT 1and GLUT 2, respectively, using CLSM: **a** IPEC-J2 control cells–SGLT 1 (green) and nuclei (blue), **b** IPEC-J2 cells, 48 h p. i. with *C. parvum* (purple, yellow arrow)–SGLT 1 (green) and nuclei (blue), **c** secondary antibody control incubated with donkey-anti-rabbit antibody only, also representative for donkey-anti-goat antibody (not shown)–nuclei (blue), **d** IPEC-J2 control cells–GLUT 2 (green) and nuclei (blue), and **e**, **f** IPEC-J2 cells, infected with *C. parvum* (purple, yellow arrow)–GLUT 2 (green) and nuclei (blue); scale bar 10 μm

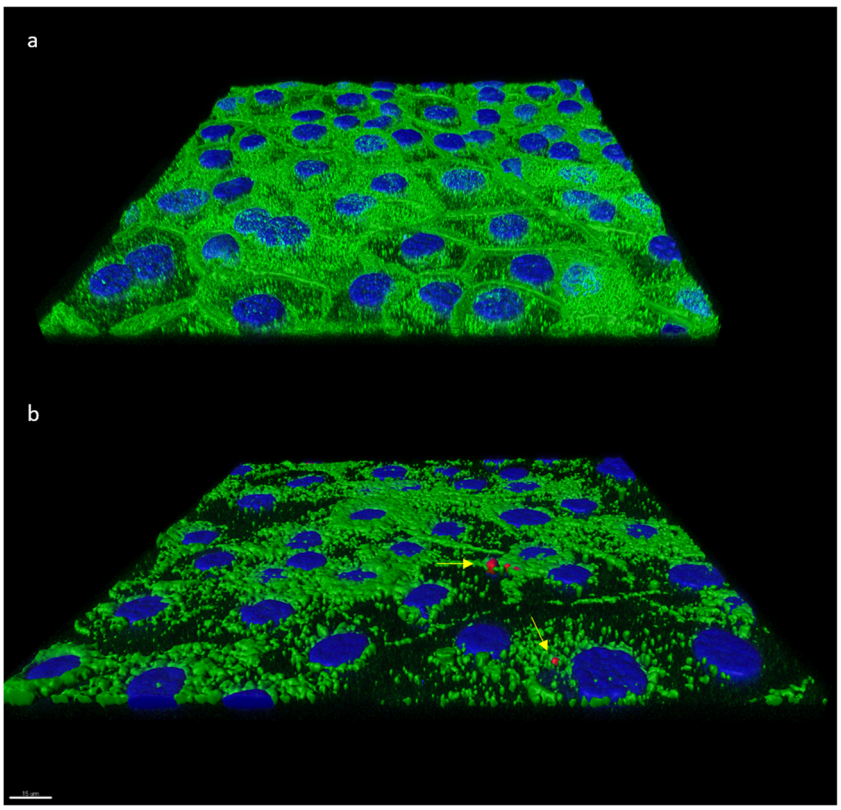

Fig. 6 3D-image of GLUT 2 localization in **a** control cells and **b** infected cells 48 h p. i. calculated from CLSM data using IMARIS™ 9.3 (Bitplane); GLUT 2 (green), nuclei (blue), and *C. parvum* (red, yellow arrow); scale bar 15 μm

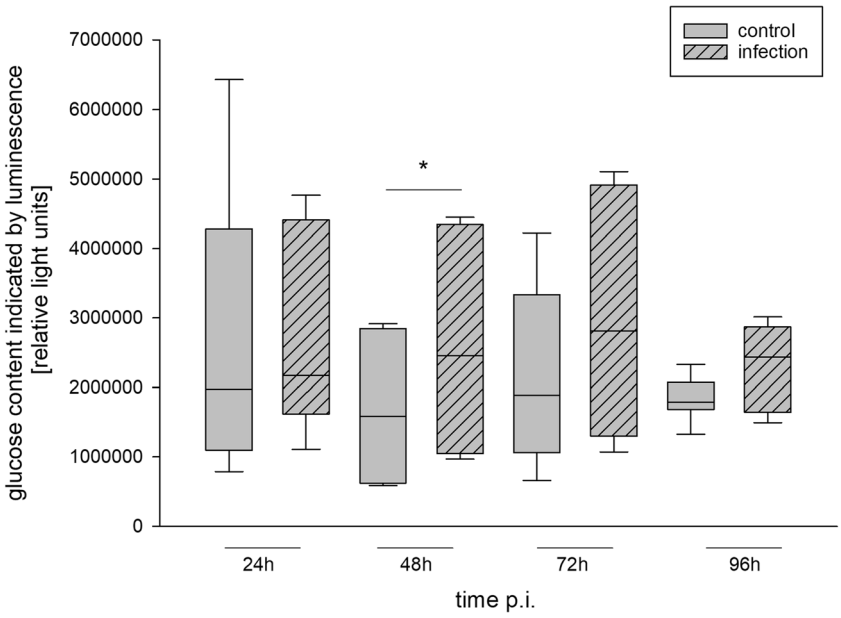

Fig. 7 Intracellular glucose level of infected cells compared with control cells 24, 48, 72, and 96 h p. i. Intracellular glucose level was detected using a luminescent assay in 8 independent experiments and compared using a paired *t* test (*$p < 0.05$)

C. parvum infection recruited host cell SGLT 1 and aquaporin (AQP) 1 to the parasite's attachment site in the cell membrane for glucose driven AQP 1 mediated water influx 1 h p. i. (Chen et al. 2005; O'Hara et al. 2010). The authors concluded that this led to an increase of cell volume and thus facilitated the cellular invasion by the parasite. In this study, no changes in total SGLT 1 protein expression were observed (Fig. 4) and no apparent changes in the subcellular localization of SGLT 1 could be detected (Fig. 5). However, it cannot be excluded that there were more pronounced differences in the subcellular localization of the transporter in the first 24 h of infection. Especially with respect to the observed upregulation of the mRNA expression of SGLT 1 at 24 h p. i. compared with noninfected cells this possibility seems feasible. After 24 h p. i., however, mRNA expression decreased gradually to a significant downregulation (Fig. 2a). This matches with earlier studies, showing a decrease in mucosal permeability and an impairment of Na^+/glucose-coupled cotransport in *C. parvum* infected suckling rats (Capet et al. 1999) and neonatal pigs (Argenzio et al. 1990) whereby absorption of other electrolytes was not significantly affected. It has also been demonstrated that Na^+/glucose-coupled cotransport was significantly diminished in *C. parvum* infected epithelium at 48 h p. i., while passive solute and macromolecular permeability in infected intestinal tissue were not significantly altered during parasite-host cell interaction 12–48 h p. i., and integrity of the epithelium was maintained at all time points (Moore et al. 1995). Thus, the initial upregulation of SGLT 1 mRNA expression could be interpreted as an attempt to normalize epithelial glucose absorption from the gut lumen and increase SGLT 1 transporter availability that is impaired in infected cells. This is often accompanied by a recruitment of other, energy-independent glucose transporters to the membrane to supplement the glucose uptake by SGLT 1 (Shepherd 2004; Kellett et al. 2008). In this study, we observed an upregulation of GLUT 1 mRNA expression which might indicate a similar mechanism in *C. parvum* infection.

Interestingly, using a microarray technology, a slight downregulation of GLUT 1 at 24 h p. i. was found (Mirhashemi et al. 2018), which seems to contradict our findings of upregulation at this early time point p. i. (Fig. 2c). However, at 96 h p. i., GLUT 1 mRNA was downregulated as well. In general, there are limitations when comparing our data with the findings of other studies, mainly due to methodological differences. It may be speculated that the sample size along with study-specific proportion of individual *C. parvum* infected cells per analyzed culture, different detection methods, and *C. parvum* strain-specific differences in virulence may be involved in partially contrary findings (Mirhashemi et al. 2018). Additionally, it was shown that results between microarray and qPCR technology can vary (Yang et al. 2010), thus, these contradictory results may be due to methodological differences. However, while the concomitant upregulation of SGLT 1 and GLUT 1 mRNA expression goes along with the increased need for glucose supply in infected cells, the general downregulation of all genes tested 96 h p. i. might be an indicator for cellular collapse after longer infection. Unfortunately, it was not possible to produce a satisfying antibody staining for GLUT 1, so in this study, no statement about the transporter's protein expression nor its localization can be given. Regarding GLUT 2, however, considerable changes in its subcellular localization were observed.

GLUT 2 is the major basolateral glucose transporter isoform in the intestine (Mueckler and Thorens 2013) and it has also been reported that a GLUT 2 translocation to the brush border membrane of the enterocytes can be induced by

cellular stress or high luminal glucose concentrations (Kellett et al. 2008). Several theories exist about the role that this transporter plays at the cell surface and it is still unclear, whether GLUT 2 serves as an additional pathway for glucose uptake or as a shunt to provide an osmotic control (Long and Cheeseman 2015). Nevertheless, a GLUT 2 trafficking to the apical membrane has also been described to be inhibited by stress, a high-fat diet, and glucocorticoids (Long and Cheeseman 2015). In the present study, a delocalization of the transporter into the cytoplasm was observed in infected cells, while in control cells, GLUT 2 was mainly present in the membrane (Figs. 5 and 6). Concomitant with this, GLUT 2 mRNA expression was significantly decreased at nearly all time points of infection. Furthermore, the strong (negative) correlation of GLUT 2 mRNA expression with the infection dose (Fig. 3) indicates a direct influence of the infection on GLUT 2 expression. Interestingly, the transporter mRNA expression in infected cells did not significantly differ from that of control cells at the peak of infection (48 h p. i.), while the protein expression was significantly increased at this time point (Fig. 4b). However, regarding the enhanced cytoplasmic localization of GLUT 2, the functionality of this protein must be questioned. The decreased mRNA expression could also be explained by the parasite's impact or by a stress response of the epithelial cells to the parasitic infection as described by others, showing a similar GLUT 2 downregulation co-occurring with a GLUT 1 upregulation in a mouse model during nematode infection (Notari et al. 2014). Lower GLUT 2 expression, both on the mRNA level and in the cell membrane, could also hint at a reduced export of hexoses. The delocalization of the transporter at 48 h p. i. indicates an intracellular reorganization induced by *C. parvum* and might also be related to the increased intracellular glucose level in infected cells.

In this study, it was shown that the intracellular glucose level in infected cells was significantly higher than in control cells 48 h p. i. Since the protein expression of SGLT 1 was not altered and a delocalization of GLUT 2 from the membrane into the cytoplasm was observed, probably an additional way of glucose uptake was used by the infected cells. In the present study, no data about the protein expression of neither GLUT 1 nor its localization in infected host cells could be collected. However, since the initially observed GLUT 1 mRNA upregulation coincided with a lower GLUT 2 mRNA expression, it may be speculated that besides supplementing SGLT 1, a compensation for GLUT 2 might be achieved by overexpression of GLUT 1 transporter as well. GLUT 1 is described to be of minor importance in the unstressed small intestinal enterocytes but may be expressed to a much higher extent under stressful conditions (Dominguez et al. 1994; Boyer et al. 1996). An upregulation of GLUT 1 mRNA expression is classically induced by hypoxia inducible factor (HIF), ensuring sufficient glucose uptake for anaerobic glycolysis and the adaptation of the cells to new metabolic challenges like hypoxia (Semenza 2011). Since the activation of HIF as an adaptive response to parasitic infection has been reported before (Spear et al. 2006; Wiley et al. 2010; Metheni et al. 2015), a regulative influence of HIF on the glucose transporters could be the underlying mechanism for the changes observed in our study.

In previous studies on parasitized mice, it has been concluded that the upregulation of GLUT 1 was induced by stress of infection compensating for the reduced activity of SGLT 1 (Sekikawa et al. 2003; Notari et al. 2014) and downregulation of GLUT 2 (Notari et al. 2014). Thus, though the data obtained in the present study do not give sufficient details to track the pathways for involvement of HIF, one may speculate that changes in GLUT 1 gene expression could support cell survival by adaption to infection stress, while securing the cellular glucose supply. As illustrated above, *C. parvum* depends on host cells' glucose supply, so the parasite might employ the enterocytes' adaptation mechanisms for its own purpose or interferes directly with the cellular glucose transport capacities. A manipulation by the parasite would be possible, since an export of parasite-derived molecules to the parasite-host interface has been shown by immunogold staining (Huang et al. 2004). Thus, it is not clear, yet, whether the herein observed changes are in favor of the parasite or the host's defense.

In conclusion, in this study, changes in the mRNA expression and protein expression of glucose transporters as well as intracellular glucose levels that hint at a cellular adaptation to the infection by *C. parvum* were observed, which may be initiated by the host or triggered by the parasite. However, the underlying signalling pathways and their possible therapeutic implications have to be addressed in further studies.

Acknowledgments The authors want to thank S. Gawlowska and I. Urbansky for excellent technical assistance.

Funding information This study was funded by a starting grant of the Faculty of Veterinary Medicine, University of Leipzig as well as the "Freundeskreis Tiermedizin der Veterinärmedizinischen Fakultät Leipzig e.V." The Leica TCS SP8 laser scanning microscope as well as the graphic work station equipped with IMARIS 9.3 was provided by the BioImaging Core Facility, University of Leipzig.

Compliance with ethical standards

Conflict of interest statement The authors declare that they have no conflict of interest.

Statement of informed consent All applicable international, national, and/or institutional guidelines for the care and use of the animals were followed. All procedures concerning the animals, which were used for the passage of the parasite, were performed in accordance with the ethical

standards of the institution (Regional Council of Saxony following German law: TierSchG, TieSchVersV; permit number: A 06/19).

References

Argenzio RA, Liacos JA, Levy ML, Meuten DJ, Lecce JG, Powell DW (1990) Villous atrophy, crypt hyperplasia, cellular infiltration, and impaired glucose-Na absorption in enteric cryptosporidiosis of pigs. Gastroenterology 98:1129–1140

Berschneider HM (1989) Development of normal cultured small intestinal epithelial cell lines which transport Na and Cl (Abstract). Gasteroenterology 96:A41

Boyer S, Sharp PA, Debnam ES, Baldwin SA, Srai SKS (1996) Streptozotocin diabetes and the expression of GLUT1 at the brush border and basolateral membranes of intestinal enterocytes. FEBS Lett 396:218–222

Bürzle M, Hediger MA (2012) Functional and physiological role of vitamin C transporters. Curr Top Membr 70:357–375. https://doi.org/10.1016/B978-0-12-394316-3.00011-9

Capet C, Kapel N, Huneau JF, Magne D, Laikuen R, Tricottet V, Benhamou Y, Tomé D, Gobert JG (1999) *Cryptosporidium parvum* infection in suckling rats: impairment of mucosal permeability and Na(+)-glucose cotransport. Exp Parasitol 91:119–125

Chen XM, O'Hara SP, Huang BQ, Splinter PL, Nelson JB, LaRusso NF (2005) Localized glucose and water influx facilitates *Cryptosporidium parvum* cellular invasion by means of modulation of host-cell membrane protrusion. Proc Natl Acad Sci U S A. 102: 6338–6343

Chen L, Tuo B, Dong H (2016) Regulation of intestinal glucose absorption by ion channels and transporters. Nutrients 8:43. https://doi.org/10.3390/nu8010043

Das S, Jayaratne R, Barrett KE (2018) The Role of Ion Transporters in the Pathophysiology of Infectious Diarrhea. Cellular and Molecular Gastroenterology and Hepatology 6 (1):33–45

Delling C, Lendner M, Müller U, Daugschies A (2017) Improvement of in vitro evaluation of chemical disinfectants for efficacy on *Cryptosporidium parvum* oocysts. Vet Parasitol 245:5–13. https://doi.org/10.1016/j.vetpar.2017.07.018

Dengler F, Rackwitz R, Pfannkuche H, Gäbel G (2017) Glucose transport across lagomorph jejunum epithelium is modulated by AMP-activated protein kinase under hypoxia. J Appl Physiol (1985) 1236:1487–1500. https://doi.org/10.1152/japplphysiol.00436.2017

Dengler F, Rackwitz R, Pfannkuche H, Gäbel G (2018) Coping with hypoxia: adaptation of glucose transport mechanisms across equine jejunum epithelium. JEVS 69:1–10

Dominguez JH, Song B, Maianu L, Garvey WT, Qulali M (1994) Gene expression of epithelial glucose transporters: the role of diabetes mellitus. J Am Soc Nephrol. 5:29–36

Dresely I, Daugschies A, Lendner M (2015) Establishment of a germ carrier assay to assess disinfectant efficacy against oocysts of coccidian parasites. Parasitol Res 114:273–281

Drinkall E, Wass MJ, Coffey TJ, Flynn RJ (2017) A rapid IL-17 response to *Cryptosporidium parvum* in the bovine intestine. Vet Immunol Immunopathol 191:1–4

Ferguson SH, Foster DM, Sherry B, Magness ST, Nielsen DM, Gookin JL (2019) Interferon-λ3 promotes epithelial defense and barrier function against *Cryptosporidium parvum* infection. Cell Mol Gastroenterol Hepatol 8:1–20. https://doi.org/10.1016/j.jcmgh.2019.02.007

Foster DM, Stauffer SH, Stone MR, Gookin JL (2012) Proteasome inhibition of pathologic shedding of enterocytes to defend barrier function requires X-linked inhibitor of apoptosis protein and nuclear factor κB. Gastroenterology 143:133–144. https://doi.org/10.1053/j.gastro.2012.03.030

Göhring F, Möller-Holtkamp P, Daugschies A, Lendner M (2014) Untersuchungen zur Häufigkeit von *Cryptosporidium parvum* bei Durchfallkälbern und der Einfluss von Koinfektionen auf das Krankheitsgeschehen. Tierärztl Umschau 69:000–000

Huang BQ, Chen XM, LaRusso NF (2004) Cryptosporidium parvum attachment to and internalization by human biliary epithelia in vitro: a morphologic study. J Parasitol 90:212–221

Kellett GL, Brot-Laroche E, Mace OJ, Leturque A (2008) Sugar absorption in the intestine: the role of GLUT2. Annu Rev Nutr 28:35–54. https://doi.org/10.1146/annurev.nutr.28.061807.155518

Kotloff KL, Nataro JP, Blackwelder WC, Nasrin D, Farag TH, Panchalingam S, Wu Y, Sow SO, Sur D, Breiman RF, Faruque AS, Zaidi AK, Saha D, Alonso PL, Tamboura B, Sanogo D, Onwuchekwa U, Manna B, Ramamurthy T, Kanungo S, Ochieng JB, Omore R, Oundo JO, Hossain A, Das SK, Ahmed S, Qureshi S, Quadri F, Adegbola RA, Antonio M, Hossain MJ, Akinsola A, Mandomando I, Nhampossa T, Acácio S, Biswas K, O'Reilly CE, Mintz ED, Berkeley LY, Muhsen K, Sommerfelt H, Robins-Browne RM, Levine MM (2013) Burden and aetiology of diarrhoeal disease in infants and young children in developing countries (the Global Enteric Multicenter Study, GEMS): a prospective, case-control study. Lancet 382:209–222

Krimi RB, Letteron P, Chedid P, Nazaret C, Ducroc R, Marie JC (2009) Resistin-like molecule-beta inhibits SGLT-1 activity and enhances GLUT2-dependent jejunal glucose transport. Diabetes 58:2032–2038. https://doi.org/10.2337/db08-1786

Lehmann A, Hornby PJ (2016) Intestinal SGLT1 in metabolic health and disease. Am J Physiol Gastrointest Liver Physiol 310:887–898. https://doi.org/10.1152/ajpgi.00068.2016

Leitch GJ, He Q (2012) Cryptosporidiosis-an overview. J Biomed Res 25: 1–16

Lendner M, Daugschies (2014) *Cryptosporidium* infections: molecular advances. Parasitology 141:1511–1532. https://doi.org/10.1017/S0031182014000237

Lendner M, Etzold M, Daugschies A (2011) Kryptosporidiose – ein Update. Berl Münch Tierärztl Wochenschr 124:10–21

Liu J, Deng M, Lancto CA, Abrahamsen MS, Rutherford MS, Enomoto S (2009) Biphasic modulation of apoptotic pathways in *Cryptosporidium parvum*-infected human intestinal epithelial cells. Infect Immun 77:837–849. https://doi.org/10.1128/IAI.00955-08

Long W, Cheeseman CI (2015) Cell Health Cytoskeleton 7:167-83

Metheni M, Lombès A, Bouillaud F, Batteux F, Langsley G (2015) HIF-1α induction, proliferation and glycolysis of *Theileria*-infected leucocytes. Cell Microbiol 17:467–472

Mirhashemi ME, Noubary F, Chapman-Bonofiglio S, Tzipori S, Huggins GS, Widmer G (2018) Transcriptome analysis of pig intestinal cell monolayers infected with *Cryptosporidium parvum* asexual stages. Parasit Vectors 11:176. https://doi.org/10.1186/s13071-018-2754-3

Moore R, Tzipori S, Griffiths JK, Johnson K, De Montigny L, Lomakina I (1995) Temporal changes in permeability and structure of piglet ileum after site-specific infection by *Cryptosporidium parvum*. Gastroenterology 108:1030–1039

Mueckler M, Thorens B (2013) The SLC2 (GLUT) family of membrane transporters. Mol Aspects Med 34:121–138. https://doi.org/10.1016/j.mam.2012.07.001

Najdrowski M, Joachim A, Daugschies A (2007) An improved in vitro infection model for viability testing of *Cryptosporidium parvum* oocysts. Vet Parasitol 150:150–154

Notari L, Riera DC, Sun R, Bohl JA, McLean LP, Madden KB, van Rooijen N, Vanuytsel T, Urban JF Jr, Zhao A, Shea-Donohue T (2014) Role of macrophages in the altered epithelial function during a type 2 immune response induced by enteric nematode infection. PLoS One 9:e84763. https://doi.org/10.1371/journal.pone.0084763 eCollection 2014

O'Hara SP, Gajdos GB, Trussoni CE, Splinter PL, LaRusso NF (2010) Cholangiocyte myosin IIB is required for localized aggregation of

sodium glucose cotransporter 1 to sites of *Cryptosporidium parvum* cellular invasion and facilitates parasite internalization. Infect Immun 78:2927–2936. https://doi.org/10.1128/IAI.00077-10

O'Hara SP, Chen X-M (2011) The cell biology of cryptosporidium infection. Microbes and Infection 13 (8-9):721–730

Pfaffl MW, Horgan GW, Dempfle L (2002) Relative expression software tool (REST) for group-wise comparison and statistical analysis of relative expression results in real-time PCR. Nucleic Acids Res 30(9):e36

Platts-Mills JA, Babji S, Bodhidatta L, Gratz J, Haque R, Havt A, McCormick BJ, McGrath M, Olortegui MP, Samie A, Shakoor S, Mondal D, Lima IF, Hariraju D, Rayamajhi BB, Qureshi S, Kabir F, Yori PP, Mufamadi B, Amour C, Carreon JD, Richard SA, Lang D, Bessong P, Mduma E, Ahmed T, Lima AA, Mason CJ, Zaidi AK, Bhutta ZA, Kosek M, Guerrant RL, Gottlieb M, Miller M, Kang G, Houpt ER (2015) MAL-ED Network Investigators. Pathogen – specific burdens of community diarrhoea in developing countries: a multisite birth cohort study (MAL-ED). Lancet Glob Health 3: e564–e575

Rider SD, Zhu G (2010) Cryptosporidium: Genomic and biochemical features. Experimental Parasitology 124 (1):2–9

Sasahara T, Maruyama H, Aoki M, Kikuno R, Sekiguchi T, Takahashi A, Satoh Y, Kitasato H, Takayama Y, Inoue M (2003) Apoptosis of intestinal crypt epithelium after *Cryptosporidium parvum* infection. J Infect Chemother. 9:278–281

Schierack P, Nordhoff M, Pollmann M, Weyrauch KD, Amasheh S, Lodemann U, Jores J, Tachu B, Kleta S, Blikslager A, Tedin K, Wieler LH (2006) Characterization of a porcine intestinal epithelial cell line for in vitro studies of microbial pathogenesis in swine. Histochem Cell Biol 125:293–305

Sekikawa S, Kawai Y, Fujiwara A, Takeda K, Tegoshi T, Uchikawa R, Yamada M, Arizono N (2003) Alterations in hexose, amino acid and peptide transporter expression in intestinal epithelial cells during *Nippostrongylus brasiliensis* infection in the rat. Int J Parasitol 33 (12):1419–1426

Semenza GL (2011) Regulation of metabolism by hypoxia-inducible factor 1. Cold Spring Harb Symp Quant Biol 76:347–353. https://doi.org/10.1101/sqb.2011.76.010678

Shepherd EJ, Helliwell PA, Mace OJ, Morgan EL, Patel N, Kellett GL (2004) Stress and glucocorticoid inhibit apical GLUT2-trafficking and intestinal glucose absorption in rat small intestine. J Physiol 560 (1):281–290

Spear W, Chan D, Coppens I, Johnson RS, Giaccia A, Blader IJ (2006) The host cell transcription factor hypoxia-inducible factor 1 is required for *Toxoplasma gondii* growth and survival at physiological oxygen levels. Cell Microbiol 8:339–352

Steinhoff-Wagner J, Zitnan R, Schönhusen U, Pfannkuche H, Hudakova M, Metges CC (2014) Diet effects on glucose absorption in the small intestine of neonatal calves: importance of intestinal mucosal growth, lactase activity, and glucose transporters. J Dairy Sci. https://doi.org/10.3168/jds.2014-8391

Tyzzer EE (1912) *Cryptosporidium parvum* (sp. nov.), a coccidium found in the small intestine of the common mouse. Arch Protistenkd 26: 394–412

Vandesompele J, De Preter K, Pattyn F, Poppe B, Van Roy N, De Paepe A, Speleman F (2002) Accurate normalization of real-time quantitative RT-PCR data by geometric averaging of multiple internal control genes. Genome Biol 3:RESEARCH0034

Wiley M, Sweeney KR, Chan DA, Brown KM, McMurtrey C, Howard EW, Giaccia AJ, Blader IJ (2010) *Toxoplasma gondii* activates hypoxia-inducible factor (HIF) by stabilizing the HIF-1α subunit via type I activing-like receptor kinase receptor signaling. J Biol Chem 285:26852–26860

Wright EM, Martín MG, Turk E (2003) Intestinal absorption in health and disease–sugars. Best Pract Res Clin Gastroenterol 17:943–956

Yang YL, Buck GA, Widmer G (2010) Cell sorting-assisted microarray profiling of host cell response to *Cryptosporidium parvum* infection. Infect Immun 78:1040–1048. https://doi.org/10.1128/IAI.01009-09

Yu Y, Zhang H, Guo F, Sun M, Zhu G (2014) A unique hexokinase in *Cryptosporidium parvum*, an apicomplexan pathogen lacking the Krebs cycle and oxidative phosphorylation. Protist 165(5):701–714. https://doi.org/10.1016/j.protis.2014.08.002

Publisher's note Springer Nature remains neutral with regard to jurisdictional claims in published maps and institutional affiliations.